

Experimental Brain Research

Coordination of muscle torques stabilizes upright standing posture: an UCM analysis

--Manuscript Draft--

Manuscript Number:				
Full Title:	Coordination of muscle torques stabilizes upright standing posture: an UCM analysis			
Article Type:	Research Article			
Funding Information:	<table border="1"> <tr> <td>National Science Foundation (0957920)</td> <td>Dr. Gregor Schöner</td> </tr> </table>	National Science Foundation (0957920)	Dr. Gregor Schöner	
National Science Foundation (0957920)	Dr. Gregor Schöner			
Abstract:	<p>The control of upright stance is commonly explained on the basis of the single-inverted pendulum model (ankle strategy), or the double inverted pendulum model (combination of ankle and hip strategy). Kinematic analysis using the Uncontrolled Manifold (UCM) approach suggests, however, that stability in upright standing results from coordinated movement of multiple joints. This is based on evidence that postural sway induces more variance in joint configurations that leave the body position in space invariant than in joint configurations that move the body in space. But does this UCM-structure of kinematic variance truly reflect coordination at the level of the neural control strategy or could it result from passive biomechanical factors? To address this question, we applied the UCM approach at the level of muscle torques rather than joint angles. Participants stood on the floor or on a narrow base of support. We estimated torques at the ankle, knee and hip joints using a model of the body dynamics. We then partitioned the joint torques into contributions from net, motion dependent, gravitational, and generalized muscle torques. A UCM analysis of the structure of variance of the muscle torque revealed that postural sway induced substantially more variance in directions in muscle torque space that leave the COM force invariant than in directions that affect the force acting on the COM. This difference decreased when we de-correlated the muscle torque data by randomizing across time. Our findings show that the UCM structure of variance exists at the level of muscle torques and is thus not merely a by-product of biomechanical coupling. Because muscle torques reflect neural control signals more directly than joint angles do, our results suggest that the control strategy for upright stance involves the task-specific coordination of multiple degrees of freedom.</p>			
Corresponding Author:	Eunse Park, Ph.D. Georgia Institute of Technology Atlanta, GA UNITED STATES			
Corresponding Author Secondary Information:				
Corresponding Author's Institution:	Georgia Institute of Technology			
Corresponding Author's Secondary Institution:				
First Author:	Eunse Park, Ph.D.			
First Author Secondary Information:				
Order of Authors:	<table border="1"> <tr> <td>Eunse Park, Ph.D.</td> </tr> <tr> <td>Hendrik Reimann, Ph.D.</td> </tr> <tr> <td>Gregor Schöner, Ph.D.</td> </tr> </table>	Eunse Park, Ph.D.	Hendrik Reimann, Ph.D.	Gregor Schöner, Ph.D.
Eunse Park, Ph.D.				
Hendrik Reimann, Ph.D.				
Gregor Schöner, Ph.D.				
Order of Authors Secondary Information:				
Author Comments:				
Suggested Reviewers:	<table border="1"> <tr> <td>Fred Danion frederic.danion@univ-amu.fr He used UCM analysis in their work.</td> </tr> <tr> <td>Allison Okamura aokamura@stanford.edu</td> </tr> </table>	Fred Danion frederic.danion@univ-amu.fr He used UCM analysis in their work.	Allison Okamura aokamura@stanford.edu	
Fred Danion frederic.danion@univ-amu.fr He used UCM analysis in their work.				
Allison Okamura aokamura@stanford.edu				

	She have used the UCM analysis
	Beth Smith beth.smith@usc.edu She used the UCM analysis for her work.
	Jianhua Wu, PhD jwu11@gsu.edu he had idea of the UCM analysis
	Mark Latash, PhD ml11@psu.edu

1
2
3
4
5
6
7
8
9
10
11
12
13
14
15
16
17
18
19
20
21
22
23
24
25
26
27
28
29
30
31
32
33
34
35
36
37
38
39
40
41
42
43
44
45
46
47
48
49
50
51
52
53
54
55
56
57
58
59
60
61
62
63
64
65

1 Coordination of muscle torques stabilizes upright standing posture: an UCM
2 analysis

3
4 Eunse Park^{1*}, Hendrik Reimann², Gregor Schöner³

5
6 ¹ Biomechanics and Movement Science

7 Univeristy of Delaware

8 Newark, DE, USA

9

10 ² Department of Kinesiology

11 Temple University

12 Philadelphia, PA, USA

13

14 ³ Institut für Neuroinformatik

15 Ruhr-Universität

16 Bochum, Germany

17

18

19 ***Contact Information**

20

21 Eunse Park

22 School of Applied physiology

23 Georgia Institution of Technology

24 555 14th St NW

25 Atlanta, GA 30332

26

27 404-894-3986 (Phone)

28 404-894-9982 (Fax)

29 eunse.park@ap.gatech.edu

30

31

32

33

34

35

36

1
2
3
4
5
6
7
8
9
10
11
12
13
14
15
16
17
18
19
20
21
22
23
24
25
26
27
28
29
30
31
32
33
34
35
36
37
38
39
40
41
42
43
44
45
46
47
48
49
50
51
52
53
54
55
56
57
58
59
60
61
62
63
64
65

37 **ABSTRACT**

38 The control of upright stance is commonly explained on the basis of the single-inverted pendulum model
39 (ankle strategy), or the double inverted pendulum model (combination of ankle and hip strategy). Kinematic analysis
40 using the Uncontrolled Manifold (UCM) approach suggests, however, that stability in upright standing results from
41 coordinated movement of multiple joints. This is based on evidence that postural sway induces more variance in
42 joint configurations that leave the body position in space invariant than in joint configurations that move the body in
43 space. But does this UCM-structure of kinematic variance truly reflect coordination at the level of the neural control
44 strategy or could it result from passive biomechanical factors? To address this question, we applied the UCM
45 approach at the level of muscle torques rather than joint angles. Participants stood on the floor or on a narrow base
46 of support. We estimated torques at the ankle, knee and hip joints using a model of the body dynamics. We then
47 partitioned the joint torques into contributions from net, motion dependent, gravitational, and generalized muscle
48 torques. A UCM analysis of the structure of variance of the muscle torque revealed that postural sway induced
49 substantially more variance in directions in muscle torque space that leave the COM force invariant than in
50 directions that affect the force acting on the COM. This difference decreased when we de-correlated the muscle
51 torque data by randomizing across time. Our findings show that the UCM structure of variance exists at the level of
52 muscle torques and is thus not merely a by-product of biomechanical coupling. Because muscle torques reflect
53 neural control signals more directly than joint angles do, our results suggest that the control strategy for upright
54 stance involves the task-specific coordination of multiple degrees of freedom.

58 **Keywords;** posture, standing, Muscle torques, uncontrolled manifold analysis

1
2
3
4
5
6
7
8
9
10
11
12
13
14
15
16
17
18
19
20
21
22
23
24
25
26
27
28
29
30
31
32
33
34
35
36
37
38
39
40
41
42
43
44
45
46
47
48
49
50
51
52
53
54
55
56
57
58
59
60
61
62
63
64
65

74 **INTRODUCTION**

75

76

Models of the control of upright stance have made simplifying assumptions. In the single inverted pendulum model (Horak, Nashner, & Diener, 1990; Jeka, Oie, Schoner, Dijkstra, & Henson, 1998; McCollum & Leen, 1989) upright standing posture is mainly controlled by activity at the ankle joint. In the double inverted pendulum model (Creath, Kiemel, Horak, Peterka, & Jeka, 2005; Loram & Lakie, 2002; Winter, Patla, Prince, Ishac, & Gielo-Perczak, 1998) upright standing postural control is achieved by the combination of ankle and hip joint activities. The ankle and hip control strategies are postulated to be always present, but one strategy may dominate depending on the difficulty of the task or the magnitude of a perturbation (Creath et al., 2005). These two control models may simplify the postural control system too much. While the contributions of the ankle and hip are important, there is evidence that other joints are recruited and coordinated to maintain upright standing posture (Hsu, Scholz, Schoner, Jeka, & Kiemel, 2007; S. Park, Horak, & Kuo, 2004; Schoner & Scholz, 2007).

86

One source of evidence is based on the idea that the variance of movement across repetitions or across time reflects the underlying control strategy (Schoner & Scholz, 2007). Variables that are stabilized by neural control mechanisms are assumed to be less variable than variables not relevant to the motor task. The uncontrolled manifold (UCM) captures those combinations of degrees of freedom that leave a hypothesized task variable invariant. In the UCM approach, for a given task variable, variance within the UCM is compared to variance orthogonal to the UCM. If variance per degree of freedom within the UCM is larger than variance orthogonal to the UCM then this is interpreted as evidence that a task variable is controlled (Scholz & Schoner, 1999). That the UCM structure of variance reveals coordination among the degrees of freedom can be determined by removing co-variance in a surrogate data set in which degrees of freedom are randomly reshuffled across time or trials (Verrel, 2011). If this destroys the UCM structure of variance, than that structure truly reflects coordination. Any remaining UCM structure of variance reflects inherent difference of variance across degrees of freedom.

97

The UCM approach has been applied to movements of the whole body from sit to stand (Scholz & Schoner, 1999; Reisman, Scholz, & Schoner, 2002). Hsu et al. (2007) applied this form of UCM analysis to the joint angles of the body during quiet stance. In a variety of conditions, they established that during quiet stance, the pattern of joint angle variance reflected the preferential stabilization of the horizontal COM or head position. Convergent evidence for such stabilization of the COM was obtained by Verrel, Lovden, and Lindenberger (2010) during walking.

102

Other evidence that multi-degree of freedom coordination is critical to upright stance comes from a study in which external mechanical perturbations are applied to a standing participant by abruptly shifting the support platform (Park et al., 2004). In an new analysis of this data, Scholz et al. (2007) showed that after a transient, postural stability was recovered in a new joint configuration which differed from the pre-perturbation configuration primarily within the UCM of the COM. In other words, following the perturbation, the mechanism of postural control reduced the deviation of the COM from its pre-perturbation position on the basis of a different, motor-equivalent joint configuration. To achieve this, the mechanism of postural control must, presumably, be sensitive to the multi-joint configuration of the upright body.

1
2
3
4
5 110 Both sources of evidence for multi-joint mechanisms of postural control are indirect. The kinematic state of
6
7 111 the body is the result of both neural signals to the skeletal musculature and the biomechanical dynamics of the multi-
8
9 112 segment body or other passive biomechanical components around the joint (e.g., elastic components of ligament,
10 113 tendon and skins). Could the kinematic patterns consistent with multi-joint coordination emerge from the
11 114 biomechanics of the upright body rather than from coordinated neural control signals to the multiple degrees of
12
13 115 freedom? One line of work that has tried to get closer to the neural control signals has consisted of detecting
14 116 coordination within the patterns of muscular activation (Krishnamoorthy, Yang, & Scholz, 2005). In this work, sets
15
16 117 of muscles are recorded during quiet stance under various conditions. The relationship between patterns of muscle
17
18 118 activation and task variables such as the COM position or Center of Pressure (COP) was estimated indirectly using a
19 119 multiple regression approach (de Freitas & Scholz, 2010). Based on the estimated Jacobian, a UCM analysis in
20 120 muscle space (or muscle mode space) became possible. Patterns of muscle synergy were discovered, in which those
21 121 combinations of muscle activations that affected the COM or COP were less variable across trials than combinations
22 122 of muscle activations that left these task variables unchanged. Similar work has established structure of variance in
23
24 123 muscle space consistent with the control of COM for isometric tasks under various conditions (Krishnamoorthy,
25
26 124 Latash, Scholz, & Zatsiorsky, 2004; Krishnamoorthy, Scholz, & Latash, 2007).

28 125 This work on muscle UCM does not really address the question we raised above, however. This form of
29
30 126 analysis establishes a direct link between patterns of muscle activation and task variables such as COM. It does not
31 127 speak to whether the coordination among joints seen at the kinematic level is caused by coordinated neural
32
33 128 commands or is a side effect of biomechanics.

34 129 Because the neural commands underlying postural control activate the muscles, and muscle activation
35
36 130 produces torques on joints, joint torques are more directly a reflection of such neural commands than are the joint
37 131 kinematics, that depend also on other biomechanical factors. In the present study we aim to establish that joint
38
39 132 torques are coordinated to control task variables at the level of the COM. Specifically, we relate joint torques to the
40 133 force acting on the COM, a task variable relevant to postural control. If such a UCM analysis of variance shows that
41 134 muscle torques are coordinated to stabilize COM force, this provides support for the hypothesis that the coordination
42
43 135 underlying the stabilization of the COM originates from neural commands and is not due primarily to the
44
45 136 biomechanical properties of the system.

46 137 Yen, Auyang, and Chang (2009) have performed a related analysis of variance at the torque level using the
47
48 138 UCM approach. The task studied was hopping in place and the task variable considered was the ground reaction
49
50 139 force in the vertical direction. We will be using a similar method for estimating the Jacobian that links forces at the
51 140 end-effector level to joint torques (Khatib, 1987) . Our analysis employs joint angles rather than the segment angles
52
53 141 used in that earlier work. We believe, that is physiologically and biomechanically more appropriate (Scholz &
54 142 Schöner, 2014). We are studying upright stance, of course, rather than hopping, and horizontal COM force rather
55
56 143 than ground reaction forces.

57 144
58
59 145 ***METHODS***
60 146
61
62
63
64
65

1
2
3
4
5
6
7
8
9
10
11
12
13
14
15
16
17
18
19
20
21
22
23
24
25
26
27
28
29
30
31
32
33
34
35
36
37
38
39
40
41
42
43
44
45
46
47
48
49
50
51
52
53
54
55
56
57
58
59
60
61
62
63
64
65

Participants:

Twelve healthy young subjects (5 males and 7 females, mean age 24.0 ± 3.8 years old) volunteered to participate in this study. They ranged from 51 to 88-kg in weight (67.2 ± 12.2 kg) and 1.52 to 1.84-m in height (170.1 ± 8.7). Subjects were excluded if they had balance disorders, including dizziness, musculoskeletal injuries and neurological disorders or uncorrected visual acuity deficits. Subjects signed an informed consent form according to the procedures approved by the Institutional Review Board of the University of Delaware in compliance with ethical standards specified by the 1964 Declaration of Helsinki.

Experimental Setup and Procedure:

A single session of data collection was conducted for each subject. Each subject performed three 3-minute trials each in two conditions: (1) Quiet standing on the normal floor (QS) and (2) Quiet standing on narrow wooden block (9-cm and 10-cm depends on the foot size) (NB). Subjects were asked to stand comfortably and to allow the body to sway naturally. Subjects were provided rest breaks as needed between trials. All trials were randomized.

Motion capture data:

Eight infrared cameras (VICON™ MX-13; Oxford Metrics) arranged in a circle around the subject were used to track the reflective markers at a sampling rate at 120-Hz. All analysis for three experiments was performed in the sagittal plane. Individual reflective markers were placed at estimated joint centers of the following locations: Lateral of 5th metatarsal bone, immediately inferior to the lateral malleolus, lateral condyle of femur, greater trochanter of femur, L5-S1 junction of spine, C7-T1 junction of spine, acromion process, mastoid process, directly anterior to the external auditory meatus.

The three-dimensional positions of the reflective markers were reconstructed with NEXUS (VICON™) software. The position information of each marker was filtered in Matlab™ using 4th order Butterworth low-pass recursive filter with a 5-Hz cut-off frequency.

Data Processing:

Reconstruction of reflective markers and kinematics:

Segment lengths and joint angles on the sagittal plane were computed for further analysis. Segment lengths (l_i) were calculated from the average of the marker positions, over the entire experimental trial. The reflective marker coordinates at each data sample were used to calculate sagittal plane vectors for the shank, thigh and trunk segments. The angles between linked segments was calculated using a link-segment model (Winter, 2009). The head and arms were included in the trunk segment, which was defined by the acromion and greater trochanter markers. The positive angle was defined as the upper (cranial) segment moving in anterior direction, based on the formula

$$\theta = \cos^{-1}(V_1^T \cdot V_2)$$

where V_1 and V_2 are unit vector for the proximal and distal segments of the joint.

After joint angle computation, joint velocities and accelerations were determined numerically by differentiating the joint angles (θ_i) using finite differences.

1
2
3
4
5
6
7
8
9
10
11
12
13
14
15
16
17
18
19
20
21
22
23
24
25
26
27
28
29
30
31
32
33
34
35
36
37
38
39
40
41
42
43
44
45
46
47
48
49
50
51
52
53
54
55
56
57
58
59
60
61
62
63
64
65

183

184 **Calculation and grouping of the joint torques:**

185

We calculated the biomechanical equation of motion using the Lagrangian approach with the joint angles as generalized coordinates:

$$M(\theta)\ddot{\theta} + C(\theta, \dot{\theta})\dot{\theta} + N(\theta) = \tau \in \mathbb{R}^3,$$

187

where $M(\theta)$ is the inertia matrix, $C(\theta, \dot{\theta})$ represents the motion-dependent torques, and $N(\theta)$ is the gravitational torques. These terms were calculated using the screw theory of spatial manipulations (Murray, Li, & Sastry, 1994).

188

189

This allowed determining the applied torques T generated by both active muscle contractions and passive elastic effects from tendons and ligaments.

190

191

These terms were grouped into torque components that are directly responsible for motions at a single joint and torques that arise from the mechanical effects of the linkage between the different joints (Galloway & Koshland, 2002). Torques in the first group are proportional to the joint accelerations,

192

193

$$NET = M_{dia}(\theta)\ddot{\theta} \in \mathbb{R}^3,$$

194

where M_{dia} is a matrix consisting of the diagonal elements of the inertia matrix. The second group consists of motion-dependent torques (MDP), which comprises terms depending upon both joint velocities and accelerations.

195

$$MDP = -M_{off}(\theta)\ddot{\theta} \in \mathbb{R}^3 - C(\theta, \dot{\theta})\dot{\theta},$$

196

Where $M_{off} = M - M_{dia}$ contains the off-diagonal elements of the inertia matrix. The remaining two groups

197

$$GRA = -N, \quad MUS = \tau$$

198

are gravitational torques (GRA) and applied torques (MUS). Both correspond directly to the terms in the equation of motion. Note that the sign for GRA and MDP was changed to make these terms directly comparable with MUS .

199

200

201 **UCM analysis:**

202

To reveal coordination between elemental variables, we applied the UCM approach (Scholz and Schoner 1999) to analyze the structure of variance relative to hypothesized task variables. When people perform any task, there is certain minimum of degrees of freedom (DOF) required to reliably solve the task. For example, 3 DOFs are required to move the hand position in 3-dimensional space. However, even considering only movements of the arm and keeping the rest of the body stationary, we have at least 7 DOF (three in the spherical shoulder, elbow flexion, radio-ulnar rotation and wrist flexion/extension and ab/adduction) to move the hand position. Because of this abundance of degrees of freedom, there are continuously many different combinations of joint angles that lead to the same spatial position of the hand. The set of these configurations that leave the hand positions unchanged is called Uncontrolled Manifold. Variance of elemental variables *within* this manifold is considered “good variance” (also designated as V_{UCM}), because it does not interfere with the hypothetical task variable. Variance that does affect the task variable, on the other hand, is called “bad variance” (V_{ORT}), because it interferes with the successful performance of a motor task. Details of the analysis can also be found in other studies (Scholz and Schoner 1999, Hsu et al. 2007, de Freitas and Scholz 2010).

215

In this study, we performed a UCM analysis using joint torques at the ankle, knee and hip in the sagittal plane

1
2
3
4
5 216 as the elemental variables, as first introduced by Yen and Chang (2009) and the force acting on the COM as task
6
7 217 variable. For comparison, we analyzed the same data using joint angles as elemental variables and the spatial COM
8
9 218 position as task variable. In both cases, UCM analysis was performed across all time frames, to determine the extent
10 219 to which each hypothetical task variable was stabilized by the CNS during postural sway.

11 220 1. We first calculated the average position of the COM (Winter, 2009). From here on, the COM is understood
12
13 221 to be the position c of this point, fixed to the trunk segment. While the actual COM position is not fixed but
14
15 222 moves relative to the trunk, the extent of this movement is negligible in quiet stance. Forces acting on this point
16 223 are not well-defined, however, which is why we used the fixed-point c instead.

17 224 2. We then calculated the kinematic Jacobian matrix J that relates changes of joint angles to changes of c . For
18
19 225 the joint torque analysis, we calculated the matrix

$$\bar{J} = M^{-1}J^T(JM^{-1}J^T)^{-1}$$

22 226 relating joint torques to forces acting on c (see Appendix and Khatib (1987)). See Figure 2 for a visualization of
23
24 227 these relationships. Both Jacobians were calculated for the mean joint angle configuration across time.

25 228 3. To approximate the UCM, we calculated the null space of these matrices and its orthogonal complement
26
27 229 using singular value decomposition in Matlab.

28 230 4. The difference between the current elemental variable configuration and its mean was projected onto the
29
30 231 null-space (UCM) and the orthogonal subspace of the Jacobian. The average lengths of these differences within
31 232 each subspace were normalized to the dimensionality of the subspace to produce estimates V_{UCM} and V_{ORT} of
32
33 233 the variance per DOF within both subspaces.

34 234
35
36 235 A difference between these variance measures ($V_{UCM} > V_{ORT}$), called a “UCM-effect”, has been interpreted as
37 236 an indication that the CNS actively controls the task variable. High stability implies low variance, so if the elemental
38
39 237 variables are actively coordinated to stabilize a relevant task variable, a UCM-effect is expected in the variance
40 238 structure of the elemental variables. While the actual observation of this UCM-effect is necessary, it is not, however,
41
42 239 a sufficient condition for active control, because the UCM-effect can also come from other sources. One such source
43 240 are intrinsic differences in the variability of the different elemental variables (Muller & Sternad, 2003; Verrel, 2011;
44
45 241 Yen & Chang, 2009). If an elemental variable that has relatively little effect on the task is intrinsically highly
46
47 242 variant, then it generates a contribution to the UCM effect that is not a result of coordination. To exclude this
48 243 possibility, we have decorrelated the data by removing the co-variation between elementary variables (Park,
49
50 244 Schoner, & Scholz, 2012; Yen & Chang, 2010). Any UCM-effect still present in the decorrelated data set cannot
51 245 result from coordination. So to determine the extent to which the observed UCM-effect result from active
52
53 246 coordination, we repeated the UCM analysis on the decorrelated data set. If V_{UCM} remains higher than V_{ORT} after
54 247 removal of the co-variation between the elemental variables, then the stabilization of the performance variable
55
56 248 originates from the coordination of the elemental variables.

57 249 58 59 250 **Statistical Analysis:**

60 251 To test whether the magnitude of variance is different between the ankle, knee and hip joints, we performed

1
2
3
4
5 252 two-factor repeated measures ANOVAs with factors *joint* and *condition*. Significance was accepted at a level of
6
7 253 $p < 0.05$. This analysis was carried out once each for joint angle variance and joint torque variance.

8 254 We performed statistical analysis of the UCM-measures of variance in joint angle and in muscle torque space,
9
10 255 before and after removing the co-variation between the elemental variables. For comparison of different UCM-
11 256 effects, we calculated the relative measure

$$\mathbf{T} = \frac{V_{UCM} - V_{ORT}}{V_{UCM} + V_{ORT}}$$

15 257 (Verrel 2010). If \mathbf{T} is close to 1, then most variance of the elemental variables preserves the task variable (Gera et
16 258 al., 2010). When \mathbf{T} is close to 0 or negative, this indicates that the task variable is not particularly stable relatively to
17 259 other combinations of degrees of freedom. Also, using a relative value makes this measure dimension-less, allows us
20 260 to compare the magnitude of UCM-effects in different spaces regardless of units (e.g. radians for angles, Nm for
21 261 torques).

23 262 Statistical analysis was used to answer four consecutive questions. 1) Is there more “good variance (V_{UCM})”
24 263 than “bad variance (V_{ORT})”? This was tested both for joint angle space and muscle torque space using a one-tailed t-
25 264 test. Significance was accepted at a level of $p < 0.025$ after Bonferroni correction. 2) Is this UCM-effect a result of
26 265 co-variation between the elemental variables or the result of differences in the intrinsic variance of the elemental
27 266 variables? We tested whether the UCM-effect is still present after removing the co-variation by performing the same
28 267 t-test on the decorrelated data set. 3) Is the reduction of the UCM-effect by decorrelating the data statistically
29 268 significant? This was tested using a t-test comparing \mathbf{T} before and after removing the co-variation, both for angles
30 269 and torques. 4) Is the UCM-effect equally large in joint angle space and in muscle torque space? This was tested
31 270 using a t-test comparing \mathbf{T} computed for joint angles and for muscle torques.

37 271 38 272 39 40 273 **RESULTS**

41 274 42 43 275 **Joint angles and torques**

44 276 *Figure 1* provides an example of torques in one quiet standing trial from one representative subject. Overall,
45 277 the magnitude of muscle torque (MUS) is similar to the gravitational torque (GRA), these two components largely
46 278 cancelling each other out at all joints. As a result, the net joint torque (NET) is comparatively small, leading to a
47 279 stable posture. As there is little movement, the motion-dependent torques (MDP) are also very small.

50 280
51
52 281 *<Figure 1 about here>*
53 282

54
55 283 *Figure 2* shows the average variance of joint angles and muscle torques for each joint, in quiet stance (light
56 284 bars) and narrow support (dark bars). The joint angle variance is smallest in the ankle compared to the knee and hip
57 285 joints. The muscle torque variance, on the other hand, is largest for the ankle and smallest for the hip. These
58 286 differences are statistically significant. The two-way repeated measures ANOVA reveals a significant effect of joint

1
2
3
4
5 287 for both joint angle variances and muscle torque variances (Joint angle variances: $F_{2,22} = 4.15, p = 0.03$; muscle
6
7 288 torque variances: $F_{2,22} = 11.15, p < 0.001$). Post-hoc testing reveals that there is no difference between ankle, knee
8
9 289 and hip joint angle variance for the quiet stance condition, but for the narrow support condition, the knee and hip
10 290 variance is significantly higher compared to the ankle variance (ankle vs. knee: $F_{1,11} = 5.18, p = 0.044$; ankle vs. hip:
11 291 $F_{1,11} = 8.33, p = 0.015$). For muscle torque variances, however, the hip variance is significantly smaller compared to
12
13 292 the variance of the ankle and knee in quiet standing (ankle vs. hip: $F_{1,11} = 9.89, p = 0.009$; knee vs. hip: $F_{1,11} = 8.45,$
14 293 $p = 0.014$) and narrow support (ankle vs. hip: $F_{1,11} = 40.04, p < 0.001$; knee vs. hip: $F_{1,11} = 18.11, p = 0.001$)
15
16 294 conditions.

17 295
18 296 *<Figure 2 about here>*
19
20 297

22 298 **Comparison of the Jacobian matrices for two UCM approaches**

23 299 *Figure 3* shows the mean across subjects of the Jacobian matrices used in the two UCM analyses for joint
24
25 300 angles and muscle torques. The pattern of these two matrices is strikingly different. In the kinematic Jacobian
26
27 301 relating joint angles to COM position, the ankle has the largest value and the hip the smallest. This is in stark
28 302 contrast to the pattern exhibited by the torque Jacobian. Here, the ankle shows the smallest (absolute) value, with a
29
30 303 larger value for the knee and an even larger value for the hip.

31 304
32 305 *<Figure 3 about here>*
33
34 306

36 307 **Variance analysis in UCM-space**

37 308 *Figure 4* shows the UCM-measures of variance V_{UCM} and V_{ORT} in joint angle space and muscle torque space,
38
39 309 before and after decorrelation, in quiet stance and narrow support. T-tests showed that in both conditions, V_{UCM} is
40 310 significantly larger than V_{ORT} for the original data in both joint angle space (QS: $p = 0.002$, NB: $p = 0.028$) and
41
42 311 muscle torque space (QS: $p = 0.001$, NB: $p = 0.004$).

43 312 After removing the covariation, no significant differences are found in joint angle space (QS: $p = 0.705$, NB:
44
45 313 $p = 0.937$). In muscle torque space, there is still a significant difference between V_{UCM} and V_{ORT} for quiet stance ($p =$
46 314 0.013), but not for the narrow support condition ($p = 0.280$).

47 315
48 316 *<Figure 4 about here>*
49
50 317

51 318 *Figure 5* shows the UCM-effect measure T for QS and NB in joint angle and muscle torque space. T is
52
53 319 significantly higher for the original data compared with the decorrelated data in both conditions in joint angle space
54 320 (QS: $p = 0.001$, NB: $p < 0.001$) and muscle torque space (QS: $p < 0.001$, NB: $p < 0.001$), suggesting that the UCM
55
56 321 effect ($V_{UCM} > V_{ORT}$) originates from active coordination of joint angles and muscle torques and is not purely a
57 322 result of the biomechanical coupling between the body segments.

58
59 323 Another t-test was performed to test the difference of T between the joint angle space and the muscle
60
61
62
63
64
65

1
2
3
4
5 324 torque space. This difference is significant for the normal data in quiet stance ($p = 0.04$), but fails to reach
6
7 325 significance in all other cases (NB with normal data: $p = 0.462$; QS with decorrelated data: $p = 0.83$; NB with
8
9 326 decorrelated data: $p = 0.147$).

10 327
11 328 *<Figure 5 about here>*
12
13 329

14 330 **DISCUSSION**

15 331 The aim of this study was to determine whether muscle torques are coordinated to stabilize COM movement
16 332 during upright standing. Our data provide evidence that the muscle torques acting on the ankle, knee and hip joints
17
18 333 in the sagittal plane are coordinated to stabilize the force acting on the COM during upright stance. These results
19 334 support the hypothesis that the coordination underlying the stabilization of the COM position originates from neural
20
21 335 commands and is not primarily due to the biomechanical coupling between the interconnected body segments.

22 336 An essential step in the UCM analysis of a high-dimensional data set is forming a hypothesis about which
23
24 337 task variable the CNS might control and determining the Jacobian matrix of partial derivatives relating changes in
25
26 338 this hypothetical task variable to changes in the elemental variables (Scholz & Schoner, 1999). In the classical UCM
27
28 339 analysis, the task variable is a function of the kinematic state of the body and the Jacobian is given by the derivative
29
30 340 of the forward kinematic function (Hsu et al., 2007; E. Park et al., 2012; Scholz & Schoner, 1999; Scholz, Schoner,
31 341 & Latash, 2000). For example, if the hypothesized task variable is the whole-body COM, the forward kinematic
32
33 342 function can be formulated using a geometrical model depending on the joint angles, segment lengths and COM
34
35 343 position of each segment.

36 344 For other task variable hypotheses, however, the relationship to the elemental variables is less
37
38 345 straightforward. A geometrical model might be excessively difficult to formulate, or not even exist. In a finger force
39 346 production task, for instance, using the finger forces as elementary variables is problematic because enslaving
40
41 347 effects between fingers compromise the mutual independence of the finger forces. Estimating the magnitude of the
42
43 348 enslavement between fingers allows to correct for this effect and derive a set of independent control variables
44
45 349 (Scholz, Danion, Latash, & Schoner, 2002; Scholz, Kang, Patterson, & Latash, 2003; Shinohara, Scholz, Zatsiorsky,
46
47 350 & Latash, 2004). In another case, the relationship between the forces exerted by the activation of the arm muscles
48
49 351 measured by EMG is highly nonlinear and complicated. It is, however, possible to approximate this relationship
50
51 352 using multiple regression analysis between the recorded force and EMG data (Danna-Dos-Santos, Slomka,
52
53 353 Zatsiorsky, & Latash, 2007; Krishnamoorthy, Goodman, Zatsiorsky, & Latash, 2003; Krishnamoorthy et al., 2007).

54 354 In the current study, we assumed that the muscle torques at the ankle, knee and hip joints are a priori
55
56 355 independent elemental variables. The hypothetical task variable that depends upon the muscle torques was the force
57
58 356 exerted on a point at the COM of the whole body. The main research question was whether the so-called UCM-
59
60 357 effect would be observed under this hypothesis, i.e. whether the vector of muscle torques is more variable in
61
62 358 directions in torque space that leave the force at the COM invariant than in directions that do affect it. The Jacobian
63
64 359 relating changes in the task variable to changes in the elemental variable was derived using an analytical formula
65
66 360 obtained for the analysis and control of robotic manipulators with respect to the dynamic behavior of the end

1
2
3
4
5 361 effector (Khatib, 1987, 1995).

6
7 362 This UCM-analysis of variance in muscle torque space was compared to the established UCM-effect in joint
8 363 angle space, which shows that joint angle combinations affecting the COM position are more stable than
9
10 364 combinations that do not (Hsu et al., 2007). Figure 3, showing the two mean Jacobian matrices of the two
11 365 approaches, illustrate the difference between these two approaches. The magnitude of the effect a joint has on the
12
13 366 task variable is *decreasing* from ankle to hip in joint angle space, but *increasing* from ankle to hip in muscle torque
14 367 space. The underlying reason behind both patterns is the relative distance of the joints from the COM of the whole
15
16 368 body. Movements of the ankle have a bigger effect on the COM than movements of the hip, because the ankle is
17 369 further away from the COM than the hip. But this also means that the lever arm translating ankle torques into forces
18
19 370 at the COM is longer, so that the same torque induces less force at the COM location for the ankle than for the hip.
20
21 371 Furthermore, the sign of the COM force Jacobian for knee torque is negative, indicating that an extensor torque at
22 372 the knee joint corresponds to a force at the COM in *backward* direction. This effect is a result of the interaction
23
24 373 torques between the different body segments. For comparison, if the knees are extended while the ankle and hip
25 374 joints are fixed, the COM moves *forward* (Zajac & Gordon, 1989). For these reasons, the structure of the data in
26
27 375 muscle torque space is expected to be different from the well-known structure of the data in joint angle space.
28
29 376

30 377 **Muscle torques are coordinated to stabilize the COM force, just like joint angles are coordinated to stabilize**
31 378 **COM position**

32
33 379 We hypothesized that both the COM position and COM force are important task related variables for upright
34 380 standing posture. When the UCM analysis was performed in joint angle space, we observed a strong UCM effect
35
36 381 (i.e., $V_{UCM} > V_{ORT}$). The means that the joint angles are coordinated to stabilize COM position to maintain upright
37 382 standing posture and this result is consistent with previous studies (Hsu & Scholz, 2011; Hsu et al., 2007; Scholz et
38
39 383 al., 2007). A similar result was found when the UCM analysis was performed with muscle torques related to the
40 384 COM force. These results indicate that regardless of the elemental variable examined (e.g., joint angles or muscle
41
42 385 torques), both are coordinated to stabilize COM movement (i.e., position and force) to maintain upright standing
43 386 posture. This is further supported by comparing the relative magnitude (T) of the UCM effect between the two UCM
44
45 387 analyses. The variance measures V_{UCM} and V_{ORT} cannot be compared directly between the two UCM analyses,
46
47 388 because they are performed on elemental variables with different units (i.e., rad vs. Nm), thus necessitating a
48
49 389 comparison of the relative difference between V_{UCM} and V_{ORT} from the two analyses (T).

50 390 This similarity of the UCM-effects suggests that the structure of postural sway in quiet stance is not a result
51 391 of biomechanical coupling between different body segments. The joint angles are strongly affected by the
52
53 392 interaction torques between interconnected body segments (Zajac & Gordon, 1989). The muscle torques, on the
54 393 other hand, mostly depend upon activation from neural control (although this relationship is not straightforward and
55
56 394 there are some passive elements involved, see e.g. Latash, 2008). Taken together these results provide support for
57 395 the hypothesis that the coordination underlying the stabilization of important task variables in postural control
58
59 396 originates from neural commands and is not primarily due to the biomechanical properties of the system.

1
2
3
4
5 397 To more completely understand whether the UCM effect (i.e., $V_{UCM} > V_{ORT}$) is due to the inter-elemental
6
7 398 variable coordination rather than the body geometry or intrinsic differences in the variability of elemental variables,
8
9 399 we artificially removed co-variation by decorrelating the data across time (Martin, Norris, Greger, & Thach, 2002;
10 400 Muller & Sternad, 2003; Yen & Chang, 2010) and then repeated the UCM analysis. If the coordination between
11 401 elemental variables plays a dominant role for the stabilization of a task variable, the UCM-effect found in the actual
12 402 data is expected to disappear, or diminish, in the decorrelated data set. In the current study, the UCM-effect indeed
13 403 largely disappeared in the decorrelated data set. This implies that the stabilization of the COM is a result of
14 404 coordination between elemental variables (i.e. joint angles or joint torques), not independent differences in
15 405 variability or body geometry. These results extend the results of previous studies, which found that the coordination
16 406 of joint angles primarily originated from the active coordination among the elemental variables (Hsu et al., 2007; E.
17 407 Park et al., 2012). For the UCM analysis in torque space a small UCM effect remained after decorrelation. This
18 408 reflects the relatively large variance of the ankle torques (Figure 2), which loads strongly on the UCM (small entry
19 409 in the Jacobian, Figure 3). The ankle torque is naturally large because the ankle faces the largest inertial moment.
20
21
22
23
24
25
26

27 411 **Conclusions**

28 412 We analyzed coordination between different joints in the control of quiet, upright stance using the
29 413 uncontrolled manifold approach at the level of muscle torques. The results provide support for the hypothesis that
30 414 muscle torques are coordinated to stabilize the force acting at the COM, analogous to the pattern of coordination
31 415 observed at the joint level. Taken together, the results from the UCM analysis on normal and decorrelated data
32 416 support the hypothesis that the geometrical structure of multi-joint postural sway in quiet stance is a result of active
33 417 coordination between different joints achieved by neural control.
34
35
36
37
38

39 419 **Acknowledgments**

40 420 We thank Darcy Reisman for useful discussions and corrections. We also thank John P. Scholz (R.I.P.) for
41 421 his effort and mentoring for the very early stage of this manuscript. This project was supported by the National
42 422 Science Foundation Grant #0957920.
43
44
45
46
47
48
49
50
51
52
53
54
55
56
57
58
59
60
61
62
63
64
65

1
2
3
4
5
6
7
8
9
10
11
12
13
14
15
16
17
18
19
20
21
22
23
24
25
26
27
28
29
30
31
32
33
34
35
36
37
38
39
40
41
42
43
44
45
46
47
48
49
50
51
52
53
54
55
56
57
58
59
60
61
62
63
64
65

434 **APPENDIX**

435
436 **The relationship between forces at the COM and joint torques**

437
438 Let x be a point on the body given by the position of the COM in reference configuration.

439 The equation of motion of the full body is given by

$$440 \quad M(\theta)\ddot{\theta} + C(\theta, \dot{\theta})\dot{\theta} + G(\theta) = \tau \quad (\text{Eq. 1})$$

441 where $M(\theta)$ is the inertia or mass matrix of the full dynamical equations of motion, $C(\theta, \dot{\theta})\dot{\theta}$ are the centrifugal and
442 Coriolis joint torques, $G(\theta)$ is gravity torque vector and τ is the vector of muscle torques. J is the kinematic
443 Jacobian relating displacement of the COM position x to changes in joint angles.

$$444 \quad \partial x = J \cdot \partial \theta \quad (\text{Eq. 2.1})$$

$$445 \quad \Leftrightarrow J = \frac{\partial x}{\partial \theta} \quad (\text{Eq. 2.2})$$

446 Our goal is to derive a matrix \bar{J} that maps torques τ to the force F applied at x via

$$447 \quad F = \bar{J}^T \tau \quad (\text{Eq. 3})$$

448 The general solution of this equation is

$$449 \quad \tau = J^T F + [I - J^T \bar{J}^T] \tau_0 \quad (\text{Eq. 4})$$

450 where τ_0 is an arbitrary joint torque vector. Together with Equation 1 we get

$$451 \quad [I - J^T \bar{J}^T] \tau_0 = M\ddot{\theta} + C + G \quad (\text{Eq. 5})$$

452 In the dynamic case with gravity, torques $[I - J^T \bar{J}^T] \tau_0$ that do not affect the endpoint force in Eq. 4 must satisfy the
453 following dynamical constraint.

$$454 \quad JM^{-1}[I - J^T \bar{J}^T] \tau_0 = 0 \quad (\text{Eq. 6})$$

455 We solve the Eq.6 for \bar{J}^T

$$456 \quad JM^{-1} \tau_0 - JM^{-1} J^T \bar{J}^T \tau_0 = 0$$

$$457 \quad JM^{-1} J^T \bar{J}^T = JM^{-1}$$

$$458 \quad \bar{J}^T = [JM^{-1} J^T]^{-1} JM^{-1} \quad (\text{Eq. 7})$$

$$459 \quad \bar{J} = M^{-1} J^T (JM^{-1} J^T)^{-1} \quad (\text{Eq. 9})$$

1
2
3
4
5 468 **REFERENCES**

- 6
7 469 Creath, R., Kiemel, T., Horak, F., Peterka, R., & Jeka, J. (2005). A unified view of quiet and perturbed
8 470 stance: simultaneous co-existing excitable modes. *Neurosci Lett*, *377*(2), 75-80. doi:
9 471 10.1016/j.neulet.2004.11.071
- 10 472 Danna-Dos-Santos, A., Slomka, K., Zatsiorsky, V. M., & Latash, M. L. (2007). Muscle modes and synergies
11 473 during voluntary body sway. *Exp Brain Res*, *179*(4), 533-550. doi: 10.1007/s00221-006-0812-0
- 12 474 de Freitas, S. M., & Scholz, J. P. (2010). A comparison of methods for identifying the Jacobian for
13 475 uncontrolled manifold variance analysis. *J Biomech*, *43*(4), 775-777. doi:
14 476 10.1016/j.jbiomech.2009.10.033
- 15 477 Galloway, J. C., & Koshland, G. F. (2002). General coordination of shoulder, elbow and wrist dynamics
16 478 during multijoint arm movements. *Exp Brain Res*, *142*(2), 163-180. doi: 10.1007/s002210100882
- 17 479 Gera, G., Freitas, S., Latash, M., Monahan, K., Schoner, G., & Scholz, J. (2010). Motor abundance
20 480 contributes to resolving multiple kinematic task constraints. *Motor Control*, *14*(1), 83-115.
- 21 481 Horak, F. B., Nashner, L. M., & Diener, H. C. (1990). Postural strategies associated with somatosensory
22 482 and vestibular loss. *Exp Brain Res*, *82*(1), 167-177.
- 23 483 Hsu, W. L., & Scholz, J. P. (2011). Motor abundance supports multitasking while standing. *Hum Mov Sci*.
24 484 doi: 10.1016/j.humov.2011.07.017
- 25 485 Hsu, W. L., Scholz, J. P., Schoner, G., Jeka, J. J., & Kiemel, T. (2007). Control and estimation of posture
27 486 during quiet stance depends on multijoint coordination. *J Neurophysiol*, *97*(4), 3024-3035. doi:
28 487 10.1152/jn.01142.2006
- 29 488 Jeka, J., Oie, K., Schoner, G., Dijkstra, T., & Henson, E. (1998). Position and velocity coupling of postural
30 489 sway to somatosensory drive. *J Neurophysiol*, *79*(4), 1661-1674.
- 31 490 Khatib, O. (1987). A Unified Approach for Motion and Force Control of Robot Manipulators - the
32 491 Operational Space Formulation. *Ieee Journal of Robotics and Automation*, *3*(1), 43-53.
- 33 492 Khatib, O. (1995). Internal Properties in Robotic Manipulation: An object-level framework. *The*
34 493 *International Journal of Robotics Research*, *14*(1).
- 35 494 Krishnamoorthy, V., Goodman, S., Zatsiorsky, V., & Latash, M. L. (2003). Muscle synergies during shifts of
36 495 the center of pressure by standing persons: identification of muscle modes. *Biol Cybern*, *89*(2),
37 496 152-161. doi: 10.1007/s00422-003-0419-5
- 38 497 Krishnamoorthy, V., Latash, M. L., Scholz, J. P., & Zatsiorsky, V. M. (2004). Muscle modes during shifts of
39 498 the center of pressure by standing persons: effect of instability and additional support. *Exp Brain*
40 499 *Res*, *157*(1), 18-31. doi: 10.1007/s00221-003-1812-y
- 41 500 Krishnamoorthy, V., Scholz, J. P., & Latash, M. L. (2007). The use of flexible arm muscle synergies to
42 501 perform an isometric stabilization task. *Clin Neurophysiol*, *118*(3), 525-537. doi:
43 502 10.1016/j.clinph.2006.11.014
- 44 503 Krishnamoorthy, V., Yang, J. F., & Scholz, J. P. (2005). Joint coordination during quiet stance: effects of
45 504 vision. *Exp Brain Res*, *164*(1), 1-17. doi: 10.1007/s00221-004-2205-6
- 46 505 Latash, M. (2008). *Neurophysiological basis of movement* (2nd ed.): Human Kinetics.
- 47 506 Loram, I. D., & Lakie, M. (2002). Human balancing of an inverted pendulum: position control by small,
48 507 ballistic-like, throw and catch movements. *J Physiol*, *540*(Pt 3), 1111-1124. doi: PHY_13077 [pii]
- 49 508 Martin, T. A., Norris, S. A., Greger, B. E., & Thach, W. T. (2002). Dynamic coordination of body parts
50 509 during prism adaptation. *J Neurophysiol*, *88*(4), 1685-1694.
- 51 510 McCollum, G., & Leen, T. K. (1989). Form and exploration of mechanical stability limits in erect stance. *J*
52 511 *Mot Behav*, *21*(3), 225-244.
- 53 512 Muller, H., & Sternad, D. (2003). A randomization method for the calculation of covariation in multiple
54 513 nonlinear relations: illustrated with the example of goal-directed movements. *Biol Cybern*, *89*(1),
55 514 22-33. doi: 10.1007/s00422-003-0399-5

- 1
2
3
4
5 515 Murray, R. M., Li, Z., & Sastry, S. S. (1994). A Mathematical introduction to Robotic Manipulation.: CRC
6 516 Press.
- 7 517 Park, E., Schoner, G., & Scholz, J. P. (2012). Functional synergies underlying control of upright posture
8 518 during changes in head orientation. *PLoS One*, *7*(8), e41583. doi: 10.1371/journal.pone.0041583
- 9 519 Park, S., Horak, F. B., & Kuo, A. D. (2004). Postural feedback responses scale with biomechanical
10 520 constraints in human standing. *Exp Brain Res*, *154*(4), 417-427. doi: 10.1007/s00221-003-1674-3
- 11 521 Reisman, D. S., Scholz, J. P., & Schoner, G. (2002). Coordination underlying the control of whole body
12 522 momentum during sit-to-stand. *Gait Posture*, *15*(1), 45-55. doi: S0966636201001588 [pii]
- 13 523 Scholz, J. P., Danion, F., Latash, M. L., & Schoner, G. (2002). Understanding finger coordination through
14 524 analysis of the structure of force variability. *Biol Cybern*, *86*(1), 29-39.
- 15 525 Scholz, J. P., Kang, N., Patterson, D., & Latash, M. L. (2003). Uncontrolled manifold analysis of single trials
16 526 during multi-finger force production by persons with and without Down syndrome. *Exp Brain*
17 527 *Res*, *153*(1), 45-58. doi: 10.1007/s00221-003-1580-8
- 18 528 Scholz, J. P., & Schoner, G. (1999). The uncontrolled manifold concept: identifying control variables for a
19 529 functional task. *Exp Brain Res*, *126*(3), 289-306.
- 20 530 Scholz, J. P., & Schöner, G. (2014). Use of the Uncontrolled Manifold (UCM) Approach to Understand
21 531 Motor Variability, Motor Equivalence, and Self-motion. In M. F. Levin (Ed.), *Progress in Motor*
22 532 *Control* (pp. 91-100): Springer New York.
- 23 533 Scholz, J. P., Schoner, G., Hsu, W. L., Jeka, J. J., Horak, F., & Martin, V. (2007). Motor equivalent control
24 534 of the center of mass in response to support surface perturbations. *Exp Brain Res*, *180*(1), 163-
25 535 179. doi: 10.1007/s00221-006-0848-1
- 26 536 Scholz, J. P., Schoner, G., & Latash, M. L. (2000). Identifying the control structure of multijoint
27 537 coordination during pistol shooting. *Exp Brain Res*, *135*(3), 382-404.
- 28 538 Schoner, G., & Scholz, J. P. (2007). Analyzing variance in multi-degree-of-freedom movements:
29 539 uncovering structure versus extracting correlations. *Motor Control*, *11*(3), 259-275.
- 30 540 Shinohara, M., Scholz, J. P., Zatsiorsky, V. M., & Latash, M. L. (2004). Finger interaction during accurate
31 541 multi-finger force production tasks in young and elderly persons. *Exp Brain Res*, *156*(3), 282-292.
32 542 doi: 10.1007/s00221-003-1786-9
- 33 543 Verrel, J. (2011). A formal and data-based comparison of measures of motor-equivalent covariation. *J*
34 544 *Neurosci Methods*, *200*(2), 199-206. doi: 10.1016/j.jneumeth.2011.04.006
- 35 545 Verrel, J., Lovden, M., & Lindenberger, U. (2010). Motor-equivalent covariation stabilizes step
36 546 parameters and center of mass position during treadmill walking. *Exp Brain Res*, *207*(1-2), 13-26.
37 547 doi: 10.1007/s00221-010-2424-y
- 38 548 Winter, D. A. (2009). *Biomechanics and motor control of human movement* (Vol. 4th). Hoboken, New
39 549 Jersey: John Wiley & Sons, Inc.
- 40 550 Winter, D. A., Patla, A. E., Prince, F., Ishac, M., & Giello-Perczak, K. (Writers). (1998). Stiffness control of
41 551 balance in quiet standing, *J Neurophysiol*.
- 42 552 Yen, J. T., Auyang, A. G., & Chang, Y. H. (2009). Joint-level kinetic redundancy is exploited to control
43 553 limb-level forces during human hopping. *Exp Brain Res*, *196*(3), 439-451. doi: 10.1007/s00221-
44 554 009-1868-4
- 45 555 Yen, J. T., & Chang, Y. H. (2009). Control strategy for stabilizing force with goal-equivalent joint torques is
46 556 frequency-dependent during human hopping. *Conf Proc IEEE Eng Med Biol Soc*, *2009*, 2115-2118.
47 557 doi: 10.1109/IEMBS.2009.5334304
- 48 558 Yen, J. T., & Chang, Y. H. (2010). Rate-dependent control strategies stabilize limb forces during human
49 559 locomotion. *J R Soc Interface*, *7*(46), 801-810. doi: 10.1098/rsif.2009.0296
- 50 560 Zajac, F. E., & Gordon, M. E. (1989). Determining muscle's force and action in multi-articular movement.
51 561 *Exerc Sport Sci Rev*, *17*, 187-230.

1
2
3
4
5 **562 Figure Captions**

6 563

7
8
9 **564 Fig 1** Example of Torques (MUS, GRA, MDP and NET) with Lagarrangian approach. This example
10 565 plotted based on one representative subject and condition, for three joints (ankle, knee and hip). MUS:
11 566 torque due to the passive and active properties of muscle. GRA: Torque due to the gravity, MDP: torque
12 567 due to motion of segments about other joints. NET: torque that is proportional to the joint acceleration.

14 568

16
17 **569 Fig 2** Variance of joints angles and muscles torques, Error bars represent standard deviation across
18 570 subjects. QS: Quiet Standing on normal floor, NB: Standing on Narrow Base of Support. *: $p < 0.05$, **: $p < 0.01$, ***: $p < 0.001$.

21 572

23
24 **573 Fig 3** The Jacobian matrixes derived from the geometrical model (left), and Jacobian derived based on the
25 574 Khatib approach (right) (1987), QS: quiet standing, NB: narrow base standing.

27 575

29
30 **576 Fig 4** The UCM results for the stabilization of COM position with respect to the joint angles (left). The
31 577 UCM results for the stabilization of COM Force with respect to the muscle torques (right). V_{UCM} :
32 578 variance of elemental variable, which does not affect the task variable, V_{ORT} : Variance of elemental
33 579 variable that does affect the task variable. QS: quiet standing, NB: narrow base standing. Norm: UCM
34 580 analysis with normal data set, De-Corr: UCM analysis with decorrelated data by removing the covariation
35 581 between elemental variables. *: $p < 0.05$, **: $p < 0.01$, ***: $p < 0.001$.

38 582

40 **583 Fig 5** Relative difference (T) between two variance components from UCM in joint angle space and
41 584 muscle torque space. QS: quiet standing, NB: narrow base standing. Norm: UCM analysis with normal
42 585 data set, De-Corr: UCM analysis with decorrelated data by removing the covariation between elemental
44 586 variables.

— MUS — GRA - - - MDP NET

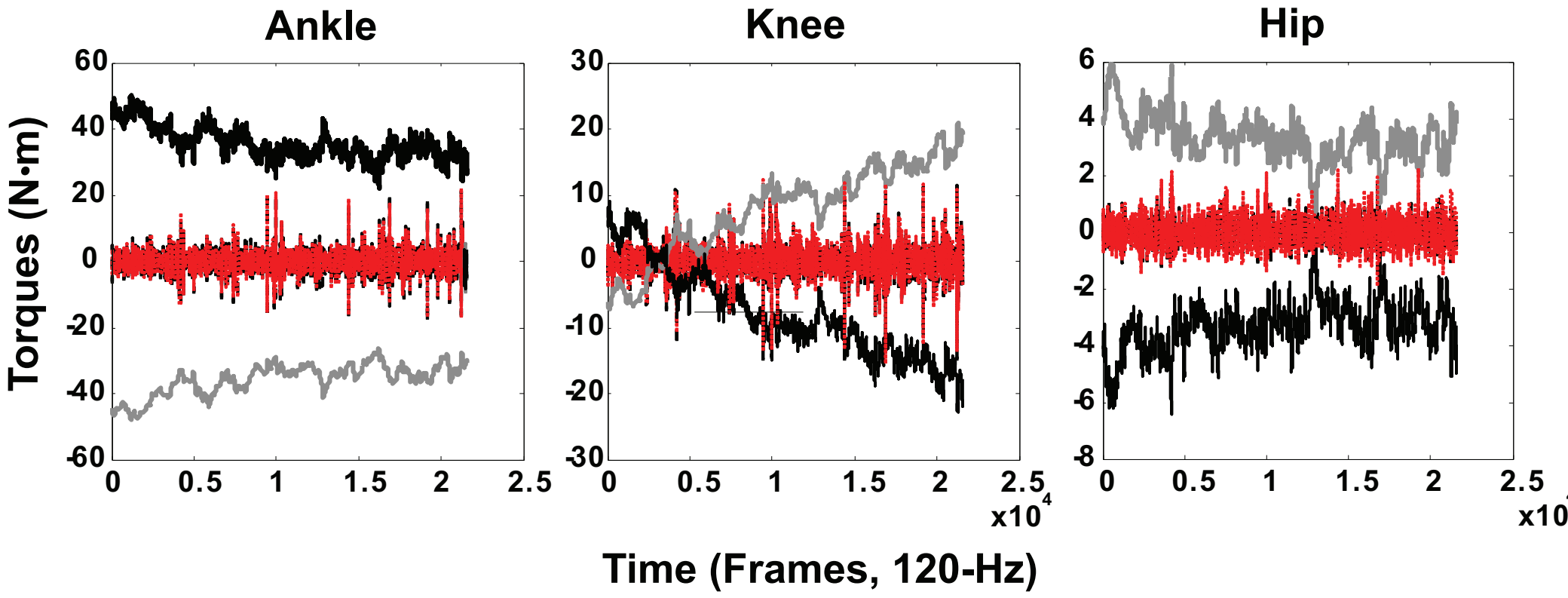


Figure 2
[Click here to download Figure: Fig2.eps](#)

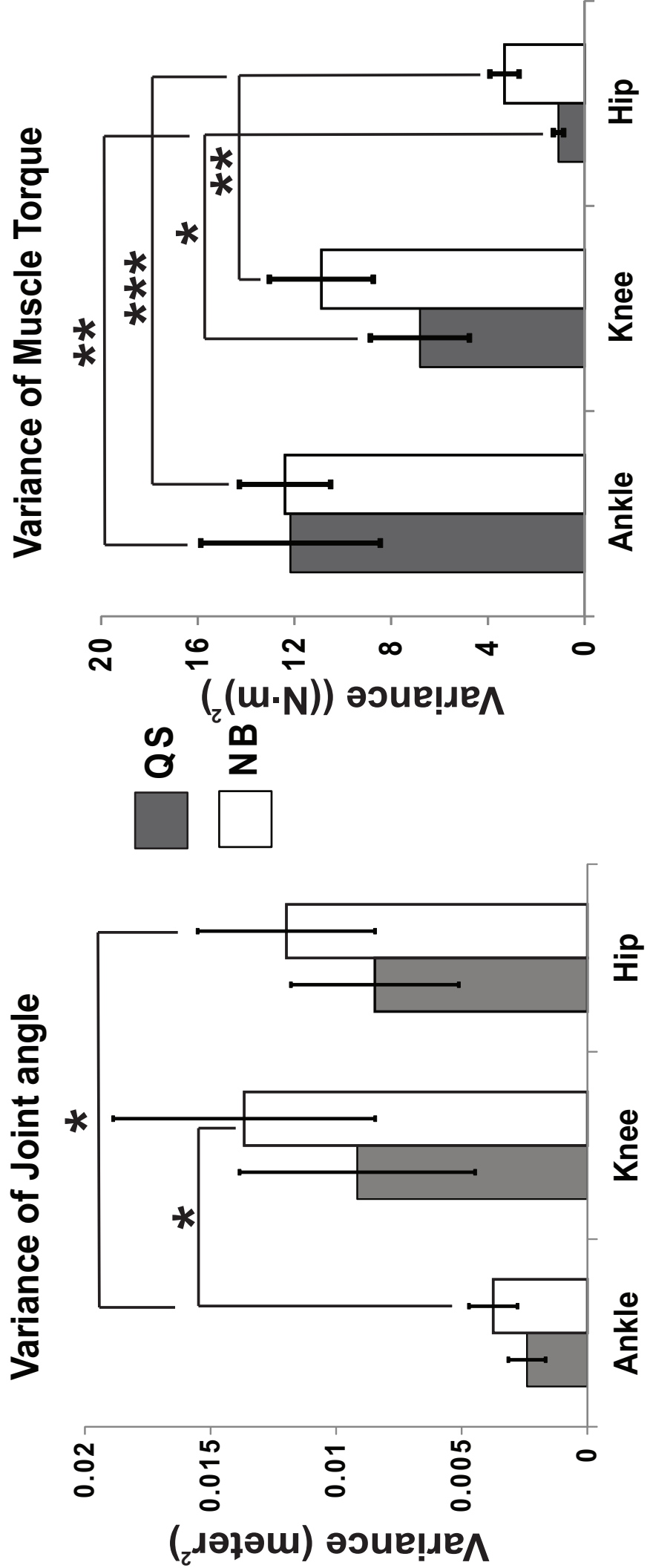
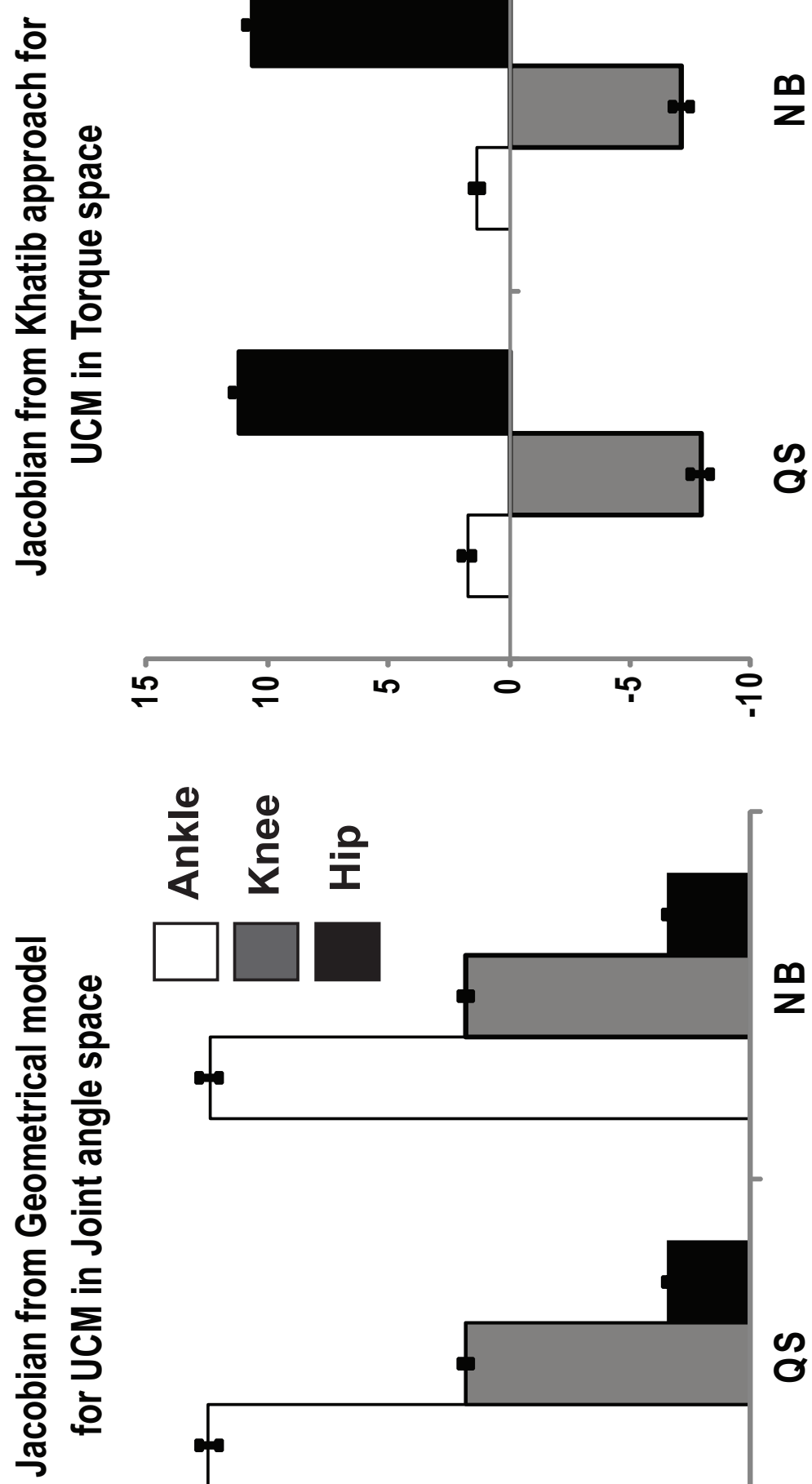
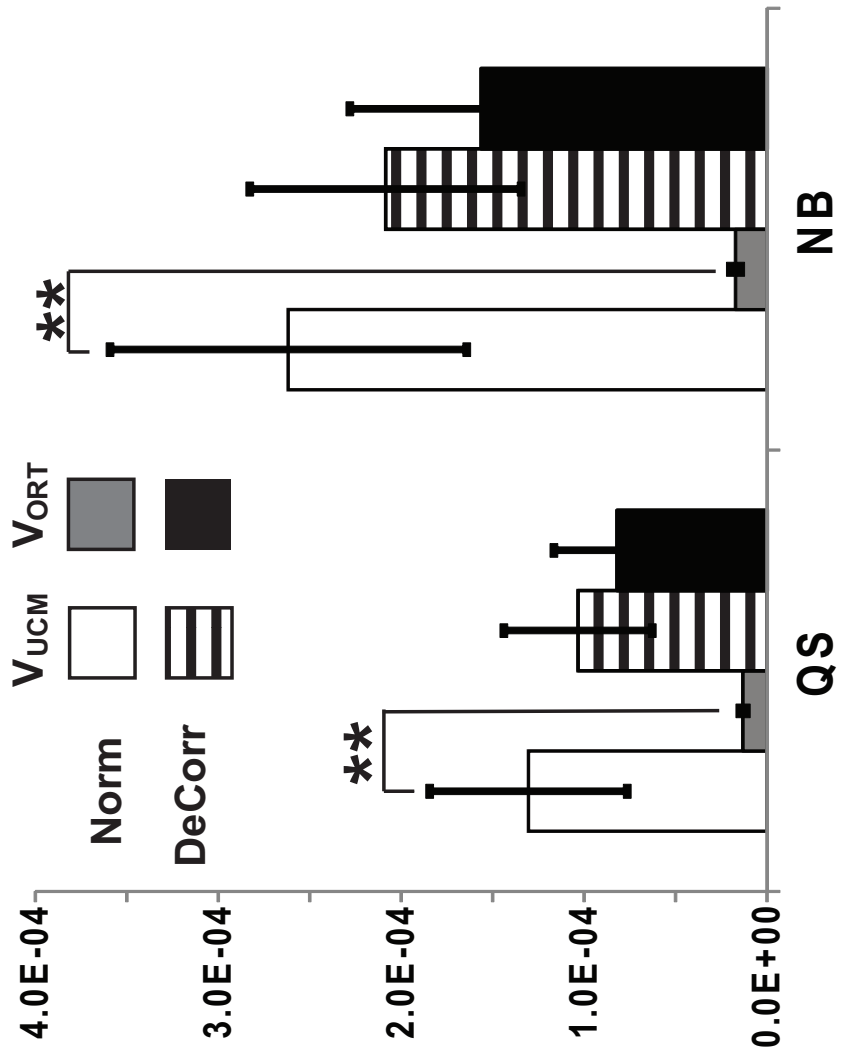


Figure 3
[Click here to download Figure: Fig3.eps](#)



UCM Analysis in joint angle space (3DoF)



UCM Analysis in torque Space (3DoF)

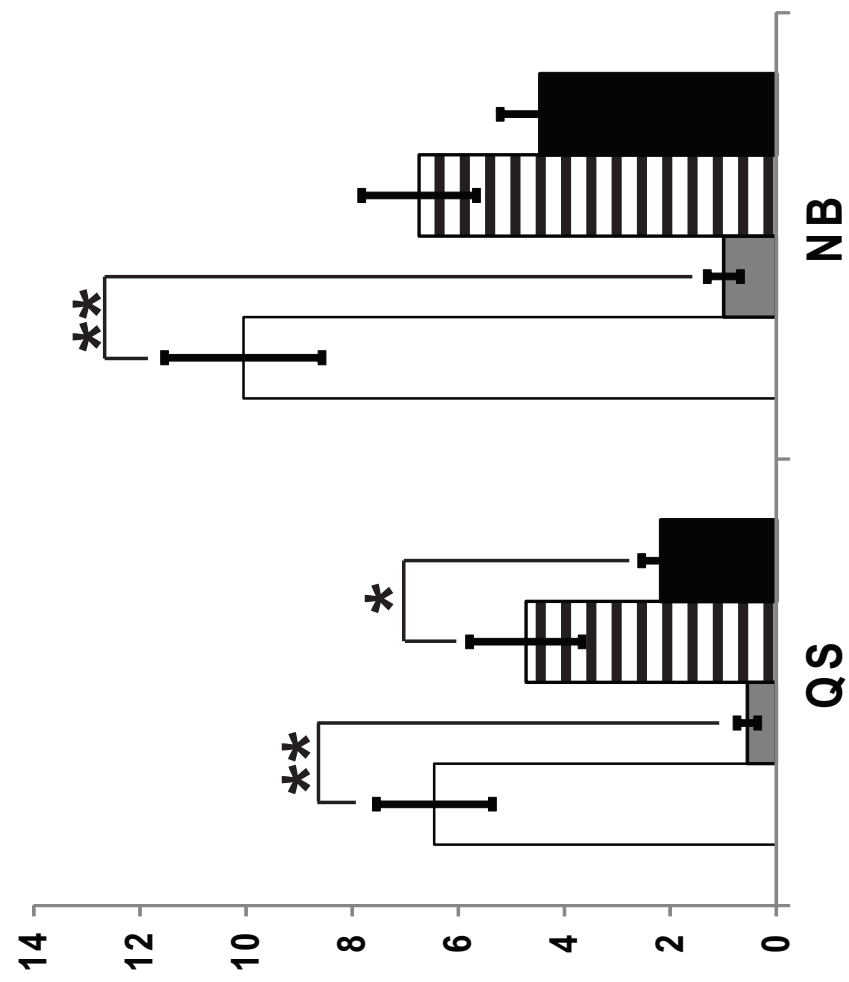


Figure 5
[Click here to download Figure: Fig5.eps](#)

